Liu-yi Li, Guo-guang Cheng, Bin Hu, Cheng-shun Wang and Guo-yu Qian*

Formation of Non-metallic Inclusions of Si-killed Stainless Steel during GOR Refining Process

https://doi.org/10.1515/htmp-2016-0188
Received August 31, 2016; accepted April 5, 2017

Abstract: The formation mechanism of inclusions in Si-killed 304 stainless steel was studied by industrial experiments during GOR refining process and thermodynamic calculations. A lager number of $CaO\text{-}SiO_2\text{-}MgO\text{-}Al_2O_3\text{-}MnO\text{-}CrO_x$ liquid spherical inclusions with different size (from 1 μm to 22 μm) had been found after deoxidization of FeSi alloy in 10 minutes. The calculation result of FactSage 6.3 software assisted in confirming that the inclusions in size of less than 5 μm that had less than 30 % CaO mainly came from the deoxidation of FeSi alloy with Ca and Al. The inclusions in size of more than 5 μm that had more than 30 % CaO mainly came from the modification of involved slag droplets through the oxidation of Si and Al and the collision with deoxidation-type inclusions, and the degree of change was bigger for smaller inclusions. The MgO in slag and refractory was reduced by Si and Al in steel, which leaded to the unceasingly increase of Mg content in steel. Subsequently, SiO_2, MnO and CrO_x in inclusion were reduced by Mg, which resulted in the increase of MgO content in inclusion and the degree of increase of MgO content was greater for the larger size of inclusions.

Keywords: stainless steel, non-metallic inclusions, formation mechanism, GOR refining, FeSi alloy

Introduction

AISI304 stainless steels are widely employed for the various usage including industry manufacture, home decoration and food and medical industry because of the excellent corrosion-resistant performance [1]. The surface quality requirement is very strict, such as the production is always very thin and a smooth and clean surface are required. However, the surface quality of stainless steel production is very sensitive to the non-metallic inclusions in steel, which can lead to the formation of surface line scale defects [2, 3]. Therefore, the control of non-metallic inclusions is very important for the production of AISI304 stainless steels. At present, the studies about the control of inclusions mainly include two aspects. The first one is the removal of inclusions by the absorption of top slag and the control of liquid steel flow pattern [4]. The second one is the modification of inclusions in order to avoid the formation of harmful inclusions based on the control of composition of both molten steel and slag [5,6, 78]. Such as the formation mechanism of spinel inclusions in stainless steel has been widely studied as a result of a formation of singular spinel (only consisting of $MgO{\cdot}Al_2O_3$) and/or of a spinel precipitation from liquid inclusions of $CaO\text{-}SiO_2\text{-}MgO\text{-}Al_2O_3$. However, there is contradiction between the removal and modification of inclusions. For example, high basicity slag is advantageous to the removal of inclusions, but it is easy to lead to the formation of $MgO{\cdot}Al_2O_3$ spinel inclusions [9]. It can be seen that the control of inclusions, such as composition, quantity and size, at the beginning of the formation is likely to become a new effective way to reduce the harm of inclusions. Therefore, it is very important for the study of source and formation mechanism of inclusions.

The predecessors' studies showed that the source of inclusions in Si-kill stainless steel mainly includes two aspects. The first one is the slag inclusions form the entrapment of top slag. The tracer was used by Kim et al. [10] to study of the source of big size inclusions (more than 20 μm) in 304 stainless steel and they found that these inclusions came from the slag entrapment. This viewpoint was substantiated by the work of Ehara et al. [11] and they also pointed out that the oxidation of Si and Al on the surface of slag inclusions can lead to the increase of SiO_2 and Al_2O_3 content, the precipitation of $MgO{\cdot}Al_2O_3$ spinel inclusions is easy when the Al_2O_3 content was more than 20 %. The works of Cha et al. [12] and Hojo et al. [13] also supported that the entrapment of top slag can lead to the formation of big size inclusions and the precipitation of $MgO{\cdot}Al_2O_3$ spinel is likely to happen even under the condition of a small

***Corresponding author: Guo-yu Qian,** State Key Laboratory of Advanced Metallurgy, University of Science and Technology Beijing, Beijing 100083, China, E-mail: qianguoyu_yejin@126.com
Liu-yi Li, State Key Laboratory of Advanced Metallurgy, University of Science and Technology Beijing, Beijing 100083, China; Southwest Stainless Steel co., LTD, Leshan, Sichuan 614000, China
Guo-guang Cheng, State Key Laboratory of Advanced Metallurgy, University of Science and Technology Beijing, Beijing 100083, China
Bin Hu, Cheng-shun Wang, Southwest Stainless Steel co., LTD, Leshan, Sichuan 614000, China

amount of Mg and Al in steel. Another source of inclusions is deoxidation of FeSi. The effect of the amount of Si addition on the composition of non-metallic inclusions in 304 stainless steel under the various condition of Si-deoxidation process was studied with the aid of the thermodynamic calculation [14], the inclusion composition changes is that $MnCr_2O_4 \rightarrow MnCr_2O_4$ + Mn-silicate→Mn-silicate→Mn-silicate + $SiO_2 \rightarrow SiO_2$ with the increase of Si content from 0 to 2%. A study was conducted by Todoroki et al. [15] to determine the effects of Al and Ca in FeSi alloy for deoxidation on inclusion composition in 18Cr-8Ni stainless steel, the result showed that Al can lead to the formation of $MgO{\cdot}Al_2O_3$ spinel and Ca can suppress its formation. However, the previous studies of the formation of inclusions were carried out only based on the consideration of a single factor, the slag entrapment or deoxidation of FeSi alloy. The formation mechanism of inclusions under the condition of these two factors has not been clear.

In the present study, the formation of inclusions and theoretic analysis for the evolution were mainly considered with industrial experiments. The characteristics of inclusions (such as morphology, number, size and composition) in steel samples taken during the process of GOR (Gas Oxygen Refining) refining were investigated under the condition of both the slag entrapment and deoxidation of FeSi alloy with Al and Ca. The formation mechanisms and evolution of different inclusions were discussed with an aid of FactSage 6.3 software and the formation mechanism of non-metallic inclusions in GOR refining process was proposed.

Experiments

Experimental procedure and sampling

In this study, the industrial experiment was made in s steel plant and the inclusions of 304 stainless steel were investigated during GOR refining. The production process of 304 stainless steel is "70 ton EAF (Electric Arc Furnace) →70 ton GOR→70 ton LF refining → Continuous casting". After oxygen blowing refining at the end of GOR refining, the first sample (NO.1) was taken from liquid steel and then was rapidly cooled in water. At the beginning of the reduction period of GOR, a certain amount of CaF_2 was added into slags for melting slag. Subsequently, some FeSi alloy was added into GOR converter for the reduction of chromic oxide in slag and deoxidation of liquid steel. The content of Si, Al and Ca in FeSi alloy is about 75%, 1.5% and 1.2%, respectively. The time of reduction period was about 10 min. The second sample (No. 2) was taken from liquid steel at the end of reduction period and a slag sample was taken at the same time, also these two samples were rapidly cooled in water. Steel and slag samples were prepared for chemical analysis.

Analysis of samples

The constituents of slag were measured by XRF analysis and the composition of slag as shown in Table 1. The major contents of steel samples were analyzed by ICP-AES (Optima ICP 7100DV) and total oxygen contents of these steel samples were measured by fusion and the infrared absorption method, the results as shown in Table 2. The inclusions of the second steel sample (No. 2) were analyzed by SEM-EDS to obtain the morphology, size and chemical compositions.

Table 1: Typical chemical composition of 304 stainless steel refining slags in GOR, wt%.

CaO	SiO_2	MgO	Al_2O_3	FeO	Cr_2O_3
50 ~ 60	28 ~ 38	4 ~ 8	0.5 ~ 2	< 1.0	0.1 ~ 1.1

Table 2: Chemical composition of 304 stainless steel, (wt%,·ppm).

Sample	C	Si	Mn	$\cdot Al_{(s)}$	$\cdot Al_{(t)}$	$\cdot Ca_{(t)}$	$\cdot Mg_{(t)}$	·T.O
No.1	0.03	< 0.01	0.40	–	–	–	–	320
No.2	0.03	0.5	1.2	10.5	24	19	5	69

Results and discussion

Morphology and chemical compositions of inclusions

Figure 1 shows the morphologies and the EDS results of four typical inclusions and the sizes of these four inclusions were 20 μm, 11 μm, 5 μm and 1.5 μm, respectively. It can be seen that the inclusions presented a spherical morphology. The main composition of the inclusions in size more than 5 μm was CaO-SiO_2-MgO-Al_2O_3 and the contents of CrO_x and MnO were very few. For the inclusions in size less than 5 μm, CaO and MgO contents increased obviously and the opposite change trend occurred for the CrO_x and MnO content. Fe element was not considered in this paper for the analysis of

inclusion composition. In addition, no other types of inclusions were found in steel samples.

The distributions of main elements of four inclusions in Figure 1 were further analyzed using EDS mapping, and the results as shown in Figure 2. It was found that all elements (such as Ca, Si, Mg, Al and O) in inclusions were distributed almost homogeneously. Therefore, the composition in the center could be considered as the composition of the entire inclusion for the composition analysis of inclusions.

The composition distribution of different inclusions in phase diagram is presented in Figure 3. Figure 3 shows that the main composition of inclusions was $CaO\text{-}SiO_2\text{-}MgO\text{-}Al_2O_3$ and the content of MgO was between 5 % and 10 %. So the $CaO\text{-}SiO_2\text{-}MgO\text{-}Al_2O_3$ quadruple phase diagram fixed MgO content of 5 % was used to determine the composition characteristics of inclusions in steel sample. It can be seen that the melting point of inclusions was lower than the temperature of liquid steel, indicating that

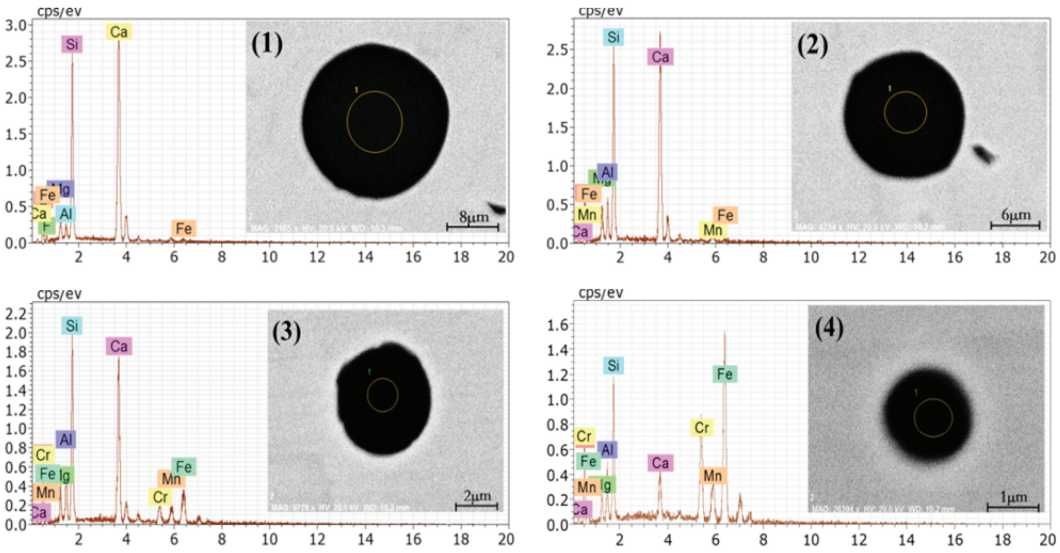

Figure 1: Morphologies and the EDS results of four typical inclusions.

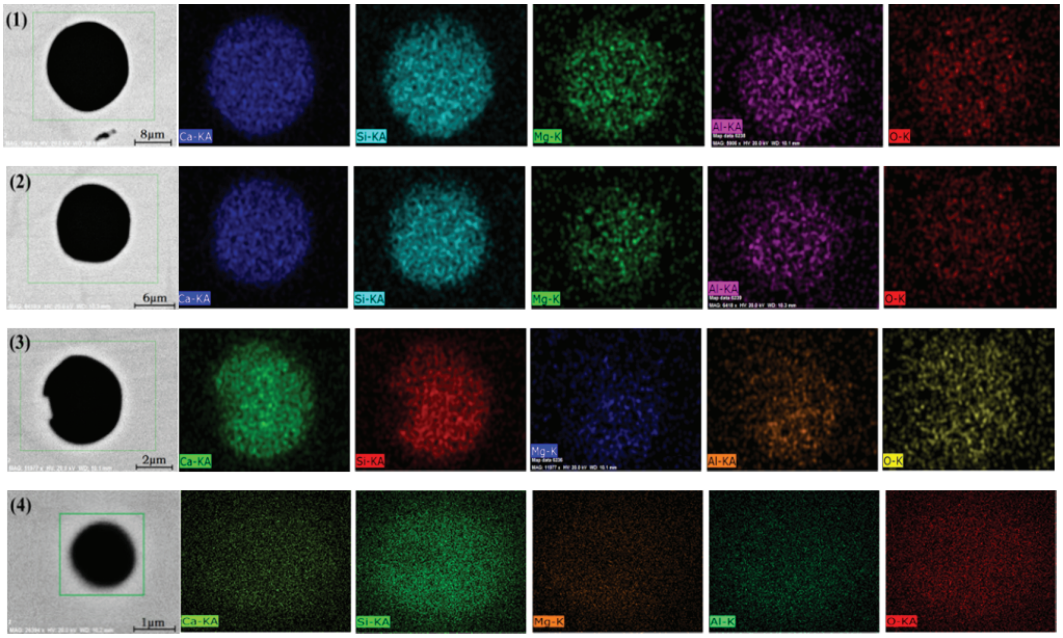

Figure 2: Distribution of main elements in different inclusions.

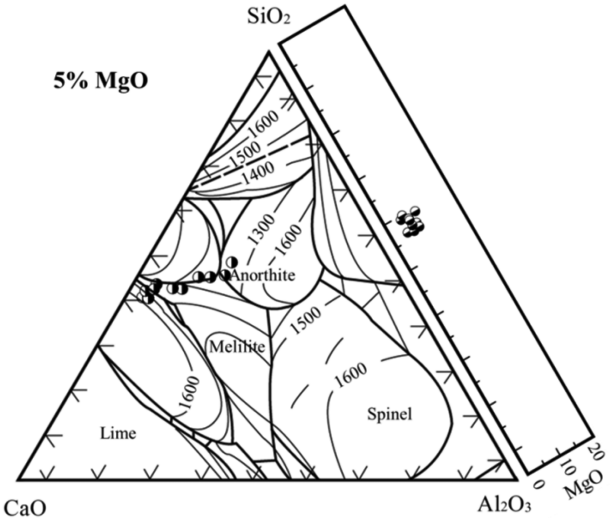

Figure 3: Phase diagram of the inclusions with size of more than 5 μm.

these inclusions were mainly exist in liquid form under the condition of steelmaking.

Corresponding relation between the size and composition of the inclusions

The change of the inclusion compositions as a function of the sizes is illustrated in Figure 4 and it can be clearly seen that the inclusion composition presented obvious change with the increase of size from 1 μm to 22 μm. Three kinds of inclusions were tried to be divided according to the relation between the size and composition, namely region (1), region (2) and region (3). The diameter of inclusions in region (3) was more than 10 μm and CaO, SiO_2, MgO and Al_2O_3 oxides content of these inclusions almost remained the same, but MnO and CrO_x almost

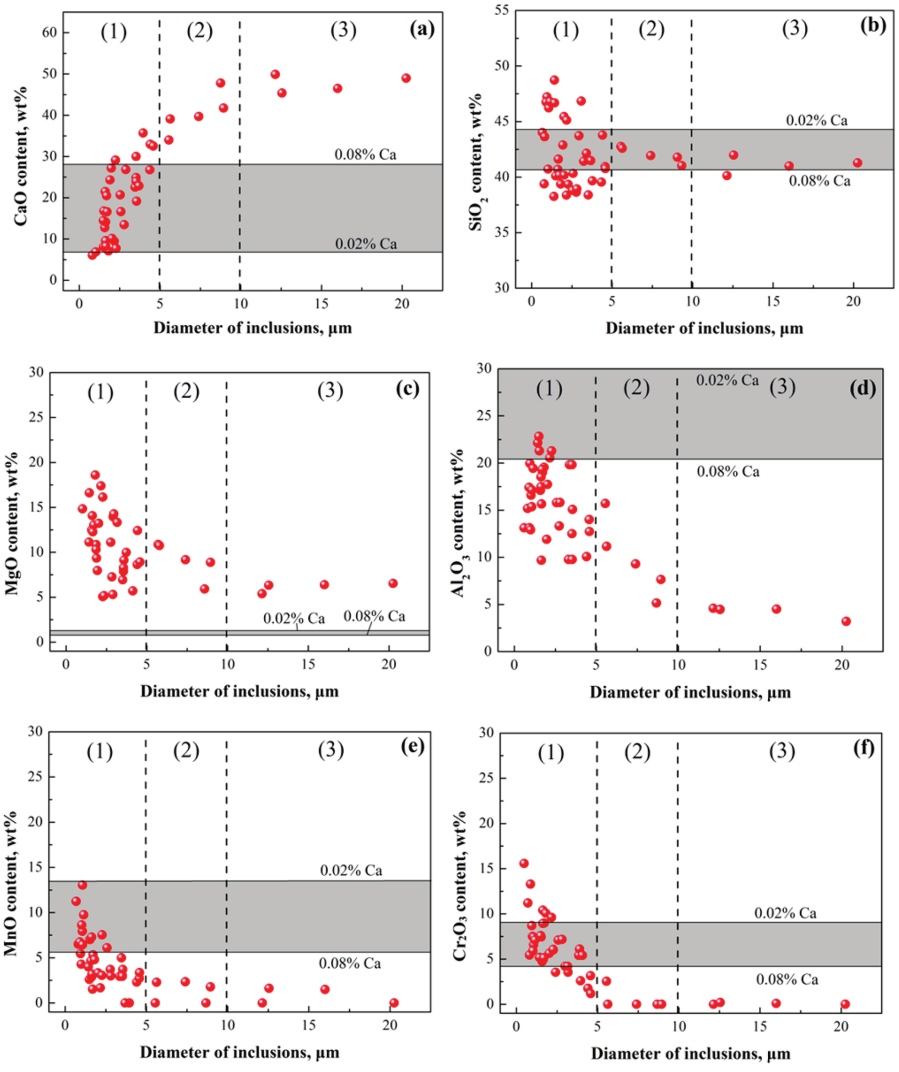

Figure 4: Comparison of inclusions between measured value and calculated value. (a) CaO, (b) SiO_2, (c) MgO, (d) Al_2O_3, (e) MnO, (f) Cr_2O_3.

were very few. The compositions of inclusion in region (1) presented an obvious change. The CaO content increased drastically from 0 to more than 30 % and both MnO and CrO_x contents decreased rapidly form 25 % to less than 5 %. The content of SiO_2, MgO and Al_2O_3 was in a wide range fluctuation. The sizes and compositions of inclusions in region (2) were between region (1) and region (3) and the oxides content of inclusions presented slow change as a function of the size.

According to the equilibrium reaction thermodynamics, a certain liquid steel content should lead to the formation of inclusions with similar composition at the same time. However, composition of inclusions in the same sample showed a larger difference. Therefore, the source and the formation process of these inclusions should be different, which would be discussed in detail in the next sections.

Calculation of chemical compositions of samples

The change of the content of molten steel is the direct cause of the change of the inclusions composition, especially for the Ca, Mg and Al high oxidizing elements, so the changes of various elements content were first confirmed.

An amount of FeSi alloy that added into GOR converter in the early stages of the recovery period was used for reducing the CrO_x of slag and deoxidation of liquid steel. The silicon content of liquid steel in recovery period of GOR was 0.5 %, indicating that the silicon content used for deoxidation was about 0.5 %. So the initial content of Al and Ca added into liquid steel could be determined based on the proportion of Si, Al and Ca in FeSi alloy, namely about 100 ppm and 80 ppm, respectively.

The corresponding relation between initial oxygen content and the equilibrium content of other elements in Fe-C-Mn-Cr-Ni–Si-Al-Ca-O at 1873 K could be calculated by using FToxid and FTmisc database of FactSage 6.3, the result as shown in Figure 5. It can be seen that equilibrium oxygen content presents a rapid decrease as the decrease of the initial oxygen content. When the initial oxygen content is less than 300 ppm, equilibrium oxygen content drops below 100ppm and the equilibrium Ca and Al content are less than 0.7 ppm and 20 ppm, respectively, indicating that Ca was almost completely consumed and Al was most oxidized during the deoxidization process of FeSi alloy.

It can be seen from Table 2 that Ca and Mg were not found in the early recovery period, but the total content of Ca and Mg increased to 19 ppm and 5 ppm in the end of recovery period, respectively. The result of Figure 7

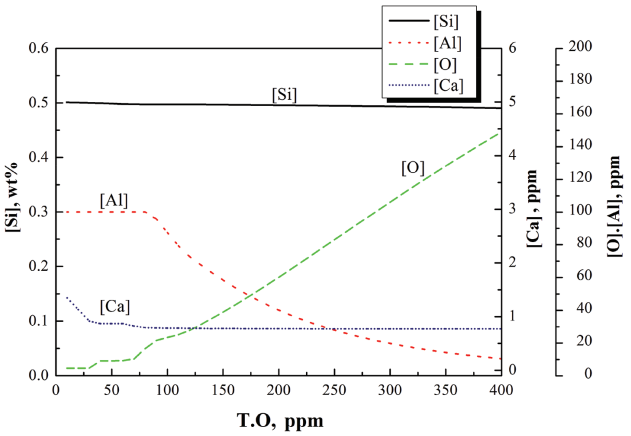

Figure 5: Effect of total oxygen on the equilibrium content of other elements.

showed that the dissolved Ca and Mg content was very rare based on the calculation of steel composition of sample No. 2 in Table 2, indicating that Ca and Mg of in the end of recovery period mainly existed in the form of oxide. The source of the total content of Ca and Mg mainly contains two aspects, namely, the form of oxide (the entrapment of slag) and the form of elemental (addition of FeSi and reduction of CaO and MgO in slag). However, it had a certain differences for the source of Ca and Mg in form of elemental. The source of Ca included drag-in of FeSi alloy and the reduction of CaO in slag, reactions as shown in eqs (1) and (2). However, the Mg mainly came from the reduction of MgO in slag or refractory, as shown in eqs (3) and (4), because that there was no Mg in FeSi.

$$3(CaO)_{slag} + 2[Al] = 3[Ca] + (Al_2O_3)_{slag} \quad (1)$$

$$2(CaO)_{slag} + [Si] = 2[Ca] + (SiO_2)_{slag} \quad (2)$$

$$3(MgO)_{slag\ or\ refractory} + 2[Al] = 3[Mg] + (Al_2O_3)_{slag\ or\ refractory} \quad (3)$$

$$2(MgO)_{slag\ or\ refractory} + [Si] = 2[Mg] + (SiO_2)_{slag\ or\ refractory} \quad (4)$$

The work of Deng and Zhu [16] showed that the Ca content only presented 0.1 % a very small increase through the reduction of slag and refractory by Al under the condition of high basicity, but the Mg content increased to 3.5 ppm a higher content. They also found that MgO in slag or and refractory was easier to be reduced by Al or Si. Park et al. [9] and Jiang et al. [17] also pointed out that the reduction of MgO was more likely to happen. Therefore, it could be confirmed that, in present study, Ca in elemental form mainly came from the drag-in of FeSi alloy in the early recovery

period and almost all Mg in elemental form continuously came into the molten steel during the process of whole reduction period due to the reduction of MgO in slag or and refractor by Al and Si.

Confirmation of equilibrium composition of inclusions

In order to find out the composition changes of inclusions investigated in sample, the inclusion composition equilibrated with molten steel must be determined firstly. Therefore, the inclusion composition as a function of the total oxygen content in Fe-0.03C-1.2Mn-18Cr -8Ni-0.04O-Si at 1873 K was calculated by using FToxid and FTmisc database of FactSage 6.3, as shown in Figure 6, the initial content of Mg and Al was set to 5 ppm and 100 ppm based on the result of Section "Calculation of chemical compositions of samples". Because of problem of the Ca yielding rate in the process of addition, 20 ppm Ca was also considered based on 25 % yielding rate [18, 20] except for initial 80 ppm Ca.

In the initial stage of recovery period, the initial oxygen content of steel sample was 320 ppm before the addition of FeSi alloy, so the 320 ppm was set to the total oxygen (T.O.) for the formation of inclusions. According to the results in Figure 6, the equilibrium composition of inclusions could be obtained under the condition of 320 ppm T.O. 20 ppm Ca and 80 ppm Ca were selected to compare with the measured value due to the uncertainty of Ca yielding rate, as shown in Figure 4. It can be seen that the calculated equilibrium values and measured values of CaO, SiO_2, MnO and Cr_2O_3 content achieved a good identical for the inclusions in region (1). For Al_2O_3 content, the calculated value was little more than measured value. The reason might be that the Al content was higher in the process of calculation due to the lack of consideration of Al yielding rate. It worth noting that the calculated value of MgO content was less than measured values, indicating that 5 ppm Mg was fail in existing in molten steel at first, and the effect of Mg on the inclusion would be discussed in Section "Effect of Mg on the inclusions composition".

For the inclusions in region (2) and region (3) according to Figure 4, there was a big deviation between the calculated value and the measured value. The change of CaO content could be well used to distinct the difference. CaO content of these inclusions was more than 30 % and the size of the inclusions was larger, the calculated equilibrium value of CaO content was more than 30 %. Two conditions were required for the increase of CaO content according to the calculated results in Figure 6, namely increasing Ca content and reducing oxygen content in the liquid steel. According to the analysis of Calculation of chemical compositions of samples, Ca from the reduction of CaO in slag was very rare, so that it was hard to support the first condition. In the practical process of deoxidation by FeSi alloy, the content of Ca and O both decreased due to the strong reaction between Ca and O [21, 22], So the content of O was impossible to increase alone, which is hard to supporting the second condition. In addition, the CaO content of inclusions with a larger size is higher, and the collision of endogenous inclusions with lower CaO content can lead to the increase of size, but fail to result in the increase of CaO content. Therefore, it could be speculated that these inclusions in region (2) and region (3) did not come from deoxidation of FeSi alloy, and mainly came from the involvement of the top slag.

Effect of slag entrapment on the formation of inclusions

The results of Section "Confirmation of equilibrium composition of inclusions" showed that the inclusions in

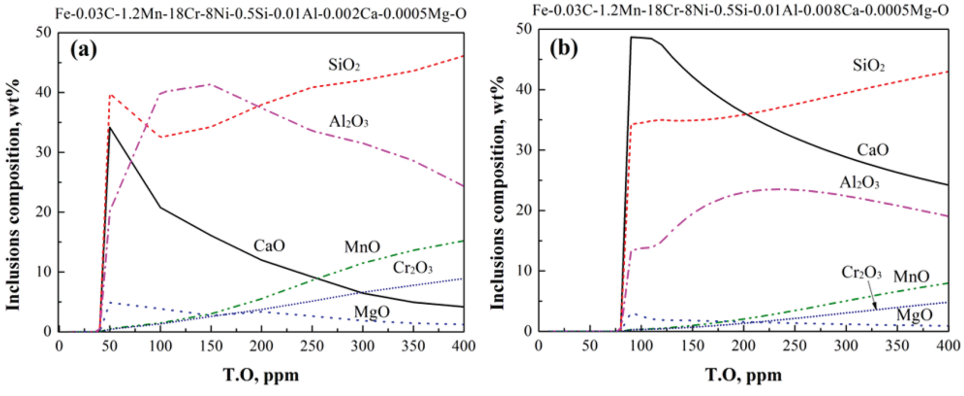

Figure 6: Inclusion composition as a function of the total oxygen content by using FactSage 6.3. (a) 0.002Ca, (b) 0.008Ca.

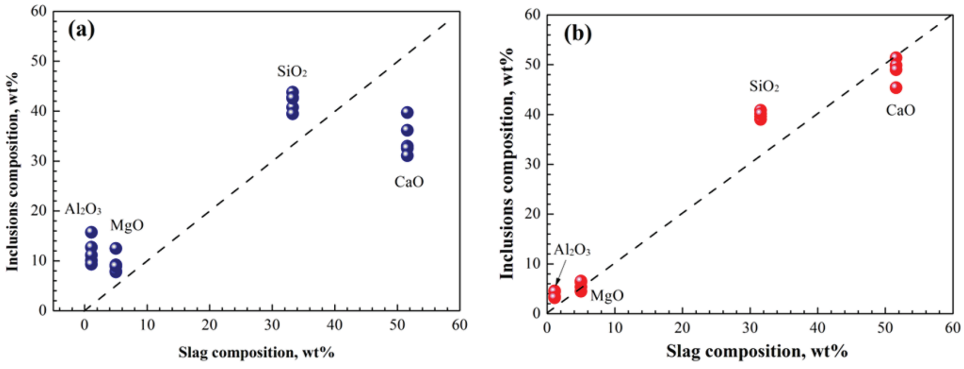

Figure 7: Comparison between slag composition and inclusions composition with different sizes. (a) 5 ~ 10 μm, (b) > 10 μm.

region (2) and region (3) might come from the involvement of the top slag, so the comparison between inclusion composition and slag composition was carried out and the result as shown in Figure 7. It can be clearly seen that the composition of the inclusions with more than 10 μm diameter was good in agree with slag composition. The content of SiO_2 and Al_2O_3 of inclusions was slightly higher than slag composition, the content of CaO was slightly lower than slag composition, but the MgO contents of inclusions and slag were almost same, indicating that the inclusions in region (2) and region (3) from the involvement of the slag. When the slag droplets got into the liquid steel, oxidation of Si and Al would occur on the surfaces of slag droplets based on the reactions of eqs (5) and (6), which could lead to the increase of SiO_2 and Al_2O_3 content and the decrease of CaO content. Ehara et al. [11] and Hojo et al. [23] also found out that oxidation of Si and Al could lead to the increase of SiO_2 and Al_2O_3 content in inclusions from slag involvement. In addition, the collision between slag type inclusions and deoxidized inclusions could further result in the increase of Al_2O_3 and SiO_2 content and the decrease of CaO content in slag type inclusions.

There was larger component difference between slag and inclusions in regional (2) than the inclusions in region (3). The reason might be the difference of the inclusion size, the oxidation of Si and Al and the collision could more easily lead to the modification of inclusions with smaller size.

$$[Si] + [O] = SiO_{2(S)}\ \Delta G^{\circ} = -576440 + 218.2T(J/mol) \quad (5)$$

$$2[Al] + 3[O] = Al_2O_{3(S)}\ \Delta G^{\circ} = -1225000 + 393.8T(J/mol) \quad (6)$$

Effect of Mg on the inclusions composition

The results of Sections “Calculation of chemical compositions of samples” and “Confirmation of equilibrium composition of inclusions” showed that the Mg mainly came from the reduction of MgO in slag or refractory after the deoxidization of FeSi alloy, so it could lead to the influence on the existing inclusions. To find out the effect of Mg on the inclusions, the inclusion composition as a function of increasing Mg content was calculated by using FToxid and FTmisc database of FactSage 6.3 based on the steel composition after deoxidization of FeSi alloy, as shown in Figure 8. It can be clearly seen that increasing Mg content could lead to the increase of MgO content and the decrease of CaO content, but the other oxides did not change obviously.

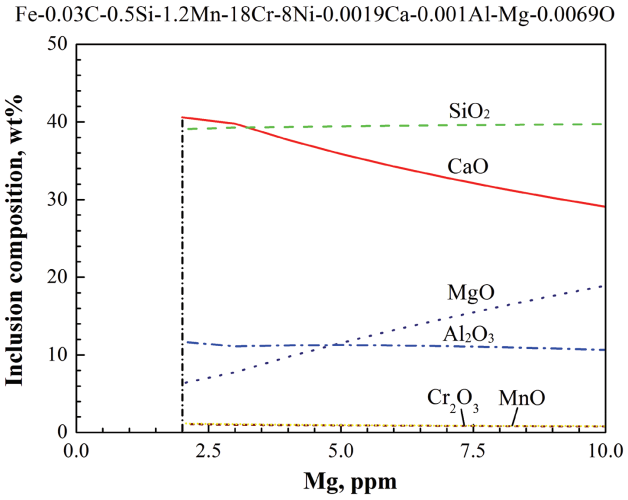

Figure 8: Composition of inclusions as a function of Mg content by using FactSage 6.5.

The calculated result confirmed that increasing Mg content could lead to the increase of MgO content, other oxides content as a function of MgO content in measured inclusions could be used to verify the effect of Mg. The inclusions in region (1) were selected because that these inclusions composition had significant fluctuation, the result as shown in Figure 9. The left picture of Figure 9

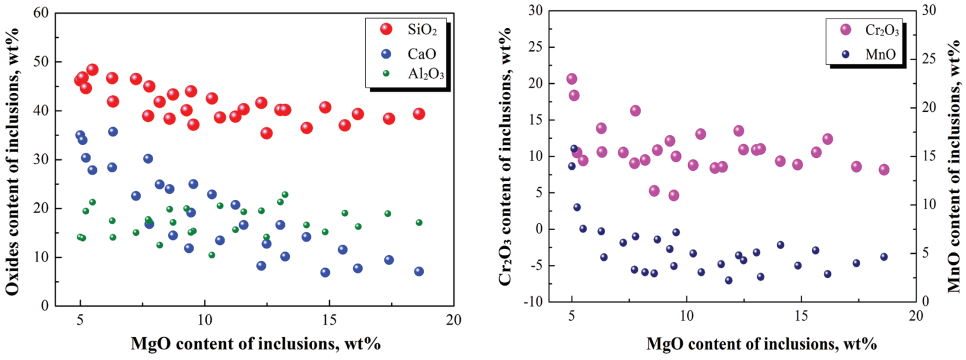

Figure 9: Inclusions composition in region (1) as a function of the MgO content inclusions.

showed that the CaO content reduced obviously with the increase of MgO content, so it could be demonstrated that Mg continuously came into the molten steel and leaded to the modification for the existing inclusions. In addition, MgO content increased cost at some SiO_2, Cr_2O_3 and MnO, based on the reactions (7) to (9), which could be used to explain the change of these oxides content in Figure 4 to some extent.

$$(SiO_2)_{Inclusions} + 2[Mg] = [Si] + 2(MgO)_{Inclusions} \quad (7)$$

$$(MnO)_{Inclusions} + [Mg] = [Mn] + (MgO)_{Inclusions} \quad (8)$$

$$(CrO_x)_{Inclusions} + x[Mg] = [Cr] + x(MgO)_{Inclusions} \quad (9)$$

For the results in Figure 4, it was worth noting that MgO content presented a trend of increase with the decrease of inclusion size. The MgO content did not change obviously for the inclusions with more than 10 µm diameter, and it increased slowly when inclusions diameter was less than 10 µm. Obviously, MgO content showed rapid increase as the diameter reduced below 5 µm. In order to find out the reason of this phenomenon, the relation between MgO content and size of inclusions was studied by the equation suggested by Okuyama [24], the rate determining step of the reaction was the mass transfer of Mg through the film in molten steel.

$$(Mg) = [Mg] \cdot L \cdot \left\{1 - exp\left(-\frac{12D_m \cdot \rho_m}{R^2 \cdot L \cdot \rho_s} \cdot t\right)\right\} \quad (10)$$

where (Mg) and [Mg] was Mg concentration of inclusion and metal at the metal-inclusion interface, respectively. L was the equilibrium distribution ratio of Mg at the metal-inclusion interface and a value of 4.0×10^5 was used as the distribution ratio [25]. D_m was the diffusion coefficient of Mg in molten steel, and a value of 3.5×10^{-9} m^2/s [25] was used. $\rho_m$and ρ_s was the density of molten steel and slag, R was the diameter of inclusion and t was the reaction time. The work of Okuyama et al. [24] showed that the reaction between Mg and inclusions was proceeding, leading a very low content of Mg in steel, so a constant value of 0.5 ppm was used [25]. As a result, the MgO content in inclusion as a function of time was obtained by the eq. (10), as shown in Figure 10. It can be seen that the degree of increase of MgO content was greater for the smaller size of inclusions at the same time.

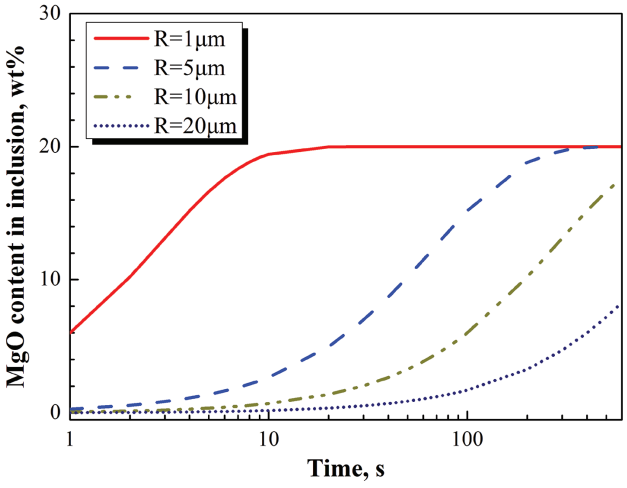

Figure 10: MgO content in inclusions as a function of time by using calculation model.

Conclusions

(1) The liquid spherical inclusions with different size were found after the deoxidation of FeSi alloy, the content of inclusions were mainly CaO-SiO_2-MgO-Al_2O_3 and the size of inclusions ranges from 1 µm to 22 µm.

(2) The inclusions in size of less than 5 µm had less than 30 % CaO content and the other oxides content of inclusions presented a fluctuation in a larger scope, and these inclusions mainly came from the deoxidation of FeSi alloy with Ca and Al according to the calculated result of FactSage 6.3 software. The

inclusions in size of more than 5 μm had more than 30 % CaO content mainly came from the involvement of the top slag. The oxidation of Si and Al and the collision with deoxidation type inclusions leaded to modification for the slag droplets, and the degree of change was bigger for smaller inclusions.

(3) The MgO in slag or and refractory was reduced by Si and Al in steel, which leaded to the unceasingly increase of Mg content in steel. Subsequently, SiO_2, MnO and CrO_x in inclusion were reduced by Mg, which resulted in the increase of MgO content in inclusion and the degree of increase of MgO content was greater for the smaller size of inclusions.

References

[1] R.C. Nunnington and N. Sutcliffe, Electric Furnace Conf. Proc., 1 (2001) 361–394.
[2] J.H. Park, D.S. Kim and S.B. Lee, *Metall. Mater. Trans. B.*, 36 (2005) 67–73.
[3] Y.Y. Bi, A.V. Karasev and P.G. Jönesson, ISIJ Int., 53 (2013) 2099–2109.
[4] Y. Ren, L.F. Zhang, W. Fang, S.J. Shao, J. Yang and W.D. Mao, Metall. Mater. Trans. B., 47 (2016) 1024–1034.
[5] P.C. Yan, S.G. Huang, L. Pandelaers, J.V. Dyck, M.X. Guo and B. Blanpain, Metall. Mater. Trans. B., 44 (2013) 1105–1119.
[6] S.K. Jo, B. Song and S.H. Kim, Metall. Mater. Trans. B., 33 (2002) 703–709.
[7] K. Fujii, T. Nagasaka and M. Hino, ISIJ Int., 40 (2000) 1059–1066.
[8] J.H. Park, Metall. Mater. Trans. B., 38 (2007) 657–663.
[9] J.H. Park and H. Todoroki, ISIJ Int., 50 (2010) 1333–1346.
[10] J.W. Kim, S.K. Kim, D.S. Kim, Y.D. Lee and P.K. Yang, ISIJ Int., 36 (1996) S140-S143.
[11] Y. Ehara, S. Yokoyama and M. Kawakami, Tetsu-to-Hagané, 93 (2007) 476–482.
[12] W.Y. Cha, D.S. Kim, Y.D. Lee and J.J. PakAK, ISIJ Int., 44 (2004) 1134–1139.
[13] M. Hojo, R. Nakao, T. Umezaki, H. Kawal, S. Tanaka and S. Fukumo, ISIJ Int., 36 (1996) S128-S131.
[14] M. Tanahashi, T. TaniguchiI, T. Kayukawa, C. Yamauchi and T. Fujisawa, Tetsu-to-Hagané, 89 (2003) 1183–1190.
[15] K. Mizuno, H. Todoroki, M. Noda and T. Tohge, Iron Steelmaker, 28 (2001) 93–101.
[16] Z.Y. Deng and M.Y. Zhu, ISIJ Int., 53 (2013) 450–458.
[17] M. Jiang, X.H. Wang and W.J. Wang, Steel Res. Int., 81 (2010) 759–765.
[18] S. Basak, R.K. Dhal and G.G. Roy, Ironmaking Steelmaking, 37 (2010) 161–168.
[19] S. Sanyal, S. Chandra and A. Singh, Trans. Indian Inst. Metals, 57 (2004) 157–169.
[20] B. Zhang, Y.M. Shi, L. Xiang, Y.Q. Chen and Y.H. Zhang, Spec. Steel., 32 (2011) 44–46.
[21] H. Iton, M. Hino and S. Ban-Ya, Tetsu-to-Hagané, 83 (1997) 695–700.
[22] J.H. Park and Y.B. Kang, Metallurgical Mater. Trans. B, 37 (2006) 791–797.
[23] K. Mineura, I. Takahashi and K. Tanak, ISIJ Int., 30 (1990) 192–198.
[24] G. Okuyama, K. Yamaguchi, S. Akeuchi and K.I. Sorimach, ISIJ Int., 40 (2002) 121–128.
[25] C. Wuppermann, A. Rückert, H. Pfeifer and H.J. Odenthal, ISIJ Int., 53 (2013) 441–449.